Novel thiophene-conjugated indoline dyes for zinc oxide solar cells

Takuya Dentani,[a] Yasuhiro Kubota,[a] Kazumasa Funabiki,[a] Jiye Jin,[b] Tsukasa Yoshida,[c] Hideki Minoura,[c] Hidetoshi Miura[d] and Masaki Matsui*[a]

Received (in Montpellier, France) 28th May 2008, Accepted 21st August 2008
First published as an Advance Article on the web 16th October 2008
DOI: 10.1039/b808959k

The application of a series of thiophene-conjugated indoline dyes for zinc oxide solar cells, prepared by the one-step cathode deposition template method, was examined. The introduction of thiophene ring(s) into **D131**-type indoline dye improved the cell performance due to their appropriate energy levels and bathochromic shift in the UV-vis absorption band on zinc oxide. It is important for the oxidation potential (E_{ox}) of dyes to have a more positive value than *ca.* 0.25 V *vs.* Fc/Fc^+ in acetonitrile in order to show a high (>70%) incident photon-to-current efficiency.

Introduction

Organic dyes, such as coumarins,[1] styryls,[2] polyenes,[3] dimethylfluorenyl-containing derivatives[4] and indoline derivatives,[5] have been reported to act as good sensitizers for titanium oxide. Bathochromic organic dyes, such as squaryliums,[6] phthalocyanines[7] and heptamethinecyanines,[8] have also been reported to sensitize semiconductors. In particular, **D149** has been reported to show the highest solar-light-to-electricity conversion efficiency (η) of 9.0% among organic dyes.[5a] One promising approach to improve the performance of sensitizers is the expansion of the π-conjugation system to absorb more photons. The introduction of ethylene and thiophene units into chromophores is a good methodology to expand π-conjugation.[9] On the other hand, a convenient preparation process for zinc oxide thin films has been reported.[10] The key point of this method is the formation of porous zinc oxide films at low temperature (<70 °C). Indoline dyes **D131**, **D102** and **D149**, in which cyanoacrylic, monorhodanic and double rhodanic acids are used as anchor moieties, respectively, are known to show good performances.[5f] We report herein the application of novel thiophene-conjugated indoline dyes having a series of anchor moieties to zinc oxide dye-sensitized solar cells.

Results and discussion

Synthesis of indoline dyes

Thiophene-conjugated indoline dyes **20–28** were synthesized, as shown in Scheme 1. Compound **1** was allowed to react with NBS (**2**) to give **3**, followed by a reaction with thiophene boronic acids esters **4–7** to provide **8–11**, which were formylated to give **12–15**. These compounds were allowed to react with cyanoacetic, mono- and double-rhodanic acids **16–19** to provide **20–28**. **D131**, **D102** and **D149** were prepared in a similar way.

UV-vis absorption and fluorescence spectra

The UV-vis absorption and fluorescence spectra of **20–28**, **D131**, **D102** and **D149** are shown in Fig. 1, Fig. 2 and Fig. 3. The results are also listed in Table 1. All the indoline dyes showed first and second absorption bands at around 500 and 400 nm, respectively. The first absorption maximum (λ_{max}^{first}) of monothiophene derivatives **20**, **23**, **24**, **25** and **26** were more bathochromic than thiophene-free derivatives **D131**, **D102** and **D149**. Interestingly, no further bathochromic shift was observed for di- and trithiophene derivatives **21**, **22**, **27** and **28** compared to monothiophene derivatives **20**, **23**, **24**, **25** and **26**, respectively. The molar absorption coefficients at the first absorption band (ε^{first}) of **20–28** were less than those of thiophene-free derivatives **D131**, **D102** and **D149**. The half-widths of **20–28** (99–146 nm) were larger than those of **D131**, **D102** and **D149** (65–79 nm). No marked difference in ε^{first} among mono-, di- and trithiophene derivatives was observed, being in the range 37 700 to 47 900. The second absorption maximum (λ_{max}^{second}) of thiophene derivatives **20–28** showed a bathochromic shift, and at the same time, their molar absorption coefficients (ε^{second}) were larger with increasing numbers of thiophene units. No remarkable differences in the UV-vis absorption spectra between **20** and **23**, and between **25** and **26**, were observed. The fluorescence maximum (F_{max}) showed a bathochromic shift by the introduction of a thiophene unit.

Electrochemical properties

The oxidation potentials (E_{ox}) of **D131**, **D102**, **D149** and **20–25** were measured by using an Ag/Ag^+ electrode in acetonitrile to compare the energy levels of E_{ox} and $E_{ox} - E_{0-0}$ of the dyes, the I^-/I_3^- potential, and the conduction band of zinc oxide.

[a] *Department of Materials Science and Technology, Faculty of Engineering, Gifu University, Yanagido, Gifu 501-1193, Japan. E-mail: matsui@apchem.gifu-u.ac.jp; Fax: +81 58 293 2794; Tel: +81 58 293 2601*
[b] *Department of Chemistry, Faculty of Science, Shinshu University, 3-1-1 Asahi, Matsumoto, Nagano 390-8621, Japan*
[c] *Environmental and Renewable Energy System Division, Graduate School of Engineering, Gifu University, Yanagido, Gifu 501-1193, Japan*
[d] *Chemicrea Co. Ltd., 2-1-6 Sengen, Tsukuba, Ibaragi 305-0047, Japan*

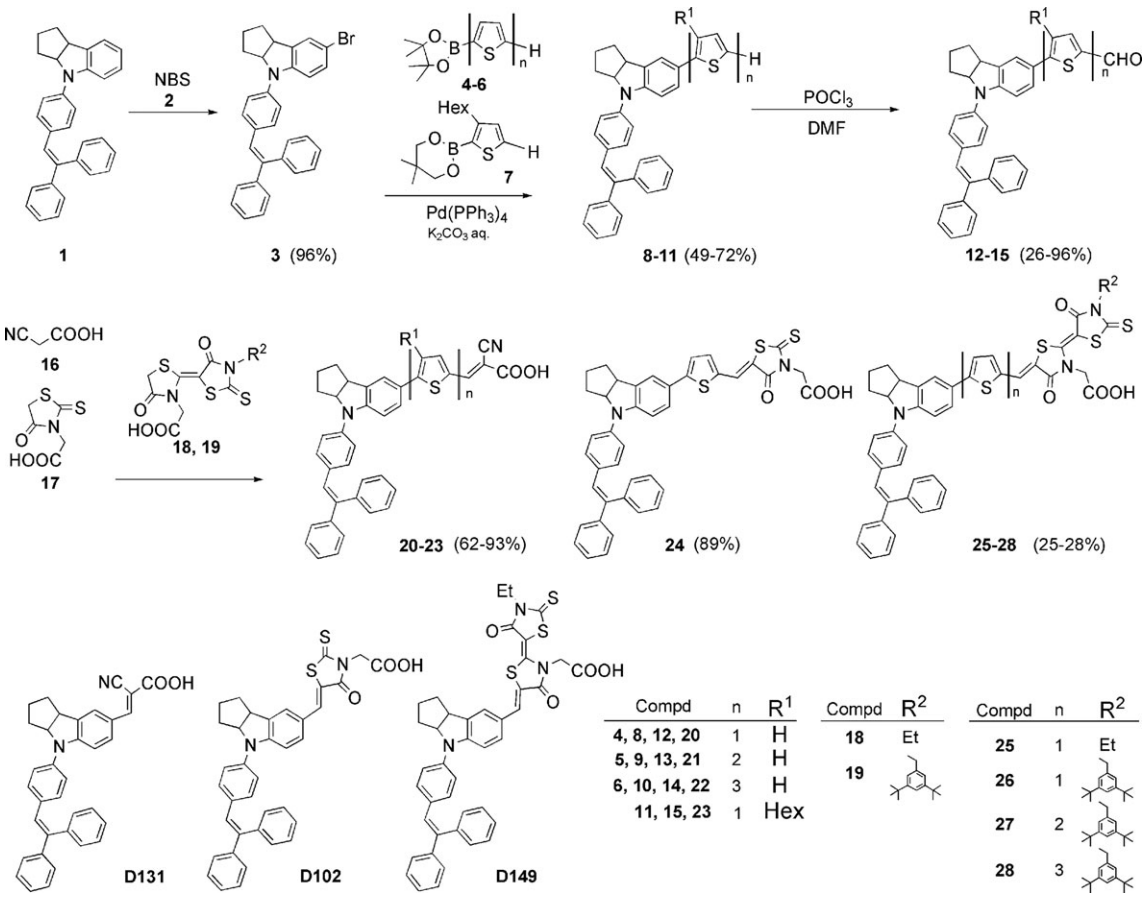

Scheme 1 The synthesis of indoline dyes **20–28**.

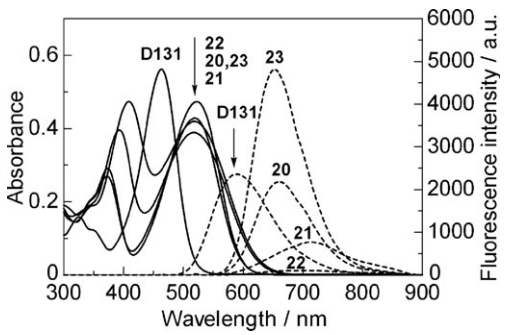

Fig. 1 UV-vis absorption and fluorescence spectra of indoline dyes **D131**, **20**, **21**, **22** and **23** at a concentration of 1.0×10^{-5} mol dm^{-3} in chloroform. Solid and dotted lines represent UV-vis absorption and fluorescence spectra, respectively.

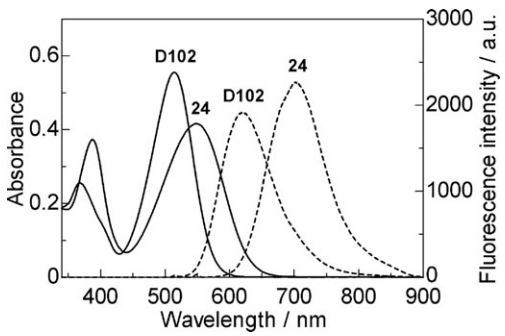

Fig. 2 UV-vis absorption and fluorescence spectra of indoline dyes **D102** and **24** at a concentration of 1.0×10^{-5} mol dm^{-3} in chloroform. Solid and dotted lines represent UV-vis absorption and fluorescence spectra, respectively.

Fc/Fc^+ was used as a standard. The E_{ox} of ferrocene was observed at $+0.13$ V *vs.* Ag/Ag^+ in acetonitrile. Fig. 4 shows that the E_{ox} of **20** was observed at $+0.38$ V *vs.* Ag/Ag^+ in acetonitrile, corresponding to $+0.25$ V *vs.* Fc/Fc^+ in acetonitrile. The I^-/I_3^- potential level was observed at $+0.09$ V *vs.* Ag/Ag^+ in acetonitrile, corresponding to -0.04 V *vs.* Fc/Fc^+ in acetonitrile.

The potential level of $E_{ox} - E_{0-0}$, where E_{0-0} represents the intersection of the normalized absorption and fluorescence spectra in solution, is considered to correspond to the LUMO energy level.[9] The E_{0-0} of **20** was observed at 589 nm, corresponding to 2.11 eV. Therefore, the $E_{ox} - E_{0-0}$ value of **20** was calculated to be -1.86 V *vs.* Fc/Fc^+ in acetonitrile. The energy levels of free indoline dyes measured in solution differed from those of adsorbed ones. Unfortunately, ferrocene and indoline dyes on a zinc oxide-coated ITO electrode did not give distinct redox responses due to a slow charge transfer process. Hence, the E_{ox} of ferrocene and indoline dyes could not be determined. The E_{ox} and $E_{ox} - E_{0-0}$ of all the indoline dyes are listed in Table 1.

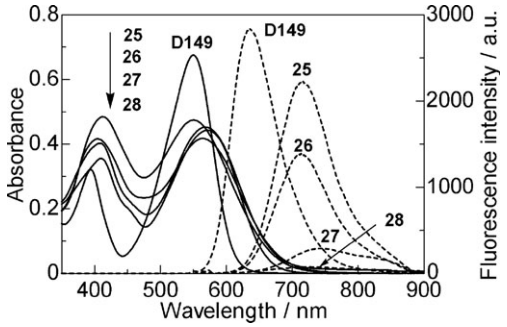

Fig. 3 UV-vis absorption and fluorescence spectra of indoline dyes **D149**, **25**, **26**, **27** and **28** at a concentration of 1.0×10^{-5} mol dm^{-3} in chloroform. Solid and dotted lines represent UV-vis absorption and fluorescence spectra, respectively.

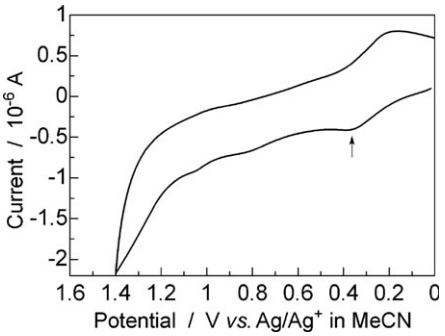

Fig. 4 The electrochemical measurement of **20** in acetonitrile (2 ml) containing tetrabutylammonium perchlorate (0.1 mol dm^{-3}). Ag/Ag$^+$ in acetonitrile was used as a reference electrode. Platinum wire was used as the working and counterelectrode. The scan rate was 100 mV s^{-1}.

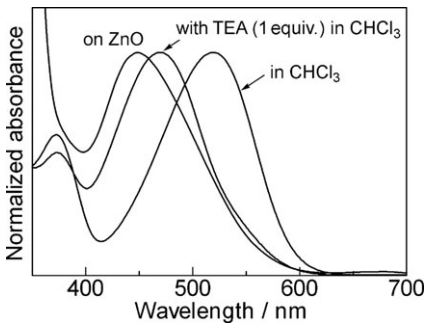

Fig. 5 The UV-vis absorption spectra of **20** in chloroform and on zinc oxide.

UV-vis absorption and IR spectra of 20

The UV-vis absorption spectra of **20** are shown in Fig. 5. The λ_{max}^{first} of **20** in chloroform and on zinc oxide were observed at 519 and 449 nm, respectively. Thus, large hypsochromic shift of λ_{max}^{first} was observed on zinc oxide. The λ_{max}^{first} of **20** in the presence of an equimolar amount of triethylamine (TEA) in chloroform was observed at 470 nm, there being slightly more bathochromic than that on zinc oxide.

FTIR spectra of **20** are shown in Fig. 6. The IR spectrum of **20** in a potassium bromide disk showed an absorption band at around 1680 cm^{-1}, which was assigned to a carbonyl stretching absorption. When indoline dye **20**, adsorbed onto a zinc oxide film, was scraped off and its IR spectrum was measured in a potassium bromide disk, the absorption band at around 1680 cm^{-1} disappeared and new absorption was observed at around 1600 cm^{-1}. This spectrum is similar to that of the triethylammonium salt of **20**, in which the absorption band at around 1600 cm^{-1} is assigned to the asymmetric stretch absorption of the carboxylate anion. It was also observed that indoline dye **20** showed negative solvatochromism in solution (λ_{max}^{first} = 516 (toluene), 519 (chloroform),

Table 1 Optical and electrochemical properties of indoline dyes

Compound	λ_{max}/nm (ε)[a]	F_{max}/nm[a]	RFI[b]	E_{ox} *vs.* Fc/Fc$^+$ in MeCN/V	$E_{ox} - E_{0-0}$ *vs.* Fc/Fc$^+$ in MeCN/V
D131	463 (55 400) 325 (15 600)	591	83	+0.41	−2.00
20	519 (43 300) 373 (27 300)	659	77	+0.25	−1.86
21	517 (37 700) 393 (38 300)	712	27	+0.23	−1.81
22	519 (41 700) 409 (47 100)	701	4	+0.22	−1.83
23	523 (47 300) 373 (29 100)	653	203	+0.25	−1.85
D102	514 (54 700) 368 (25 200)	621	68	+0.37	−1.83
24	548 (41 400) 388 (37 100)	702	80	+0.25	−1.75
D149	550 (68 000) 395 (32 000)	636	100	+0.30	−1.79
25	571 (43 500) 410 (34 800)	717	78	+0.24	−1.67
26	568 (45 600) 408 (40 500)	713	49	—[c]	—[c]
27	564 (42 000) 405 (41 900)	743	10	—[c]	—[c]
28	550 (47 900) 412 (48 900)	727	3	—[c]	—[c]

[a] Measured on 1.0×10^{-5} mol dm^{-3} of substrate in chloroform at 25 °C. [b] Relative fluorescence intensity. [c] Not measured due to low solubility.

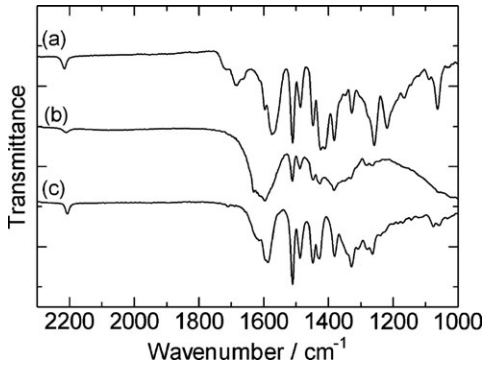

Fig. 6 FTIR spectra of **20**: (a) **20**, (b) **20** in the presence of zinc oxide and (c) the triethylammonium salt of **20**.

529 (dichloromethane), 465 (DMSO), 453 (acetonitrile) and 464 nm (methanol)). These results indicate that the hypsochromic shift of **20** on zinc oxide is mainly attributed to the formation of a bidentate complex between the carboxylate and zinc. The polar zinc oxide surface could also be attributed to the hypsochromic shift.

Photoelectrochemical properties

The cell performance of **D131**-type indoline dyes was examined. The normalized UV-vis absorption spectra on zinc oxide and action spectra are shown in Fig. 7. The results are also listed in Table 2. The cell performance was improved in the presence of cholic acid (CA), a co-adsorbate that can inhibit the aggregation of dyes on zinc oxide due to carboxylic acid and hydrophobic moieties. The UV-vis absorption spectra of **20** and **23** in the absence and presence of CA are depicted in Fig. 7(a). In the case of **20**, a broad absorption at around 530 nm decreased in the presence of CA, indicating the prevention of aggregation on zinc oxide. Meanwhile, only slight differences in the absorption bands between the absence and presence of CA were observed for **23**. The η values of **20** and **23** in the absence of CA were 3.13 and 3.30%, respectively (Table 2, runs 3 and 7). Those in the presence of CA were 3.78 and 3.36%, respectively (Table 2, runs 2 and 6). Thus, the η values of **20** and **23** were improved by 21 and 2% in the presence of CA, respectively. These results suggest that the hexyl group in **23** is very effective in inhibiting aggregation on zinc oxide. In the cases of **21** and **22**, aggregation formation decreased in the presence of CA, resulting in an improved cell performance (Table 2, runs 4 and 5). The absorption bands of **20**, **21**, **22** and **23** on zinc oxide were more bathochromic than that of **D131**, as shown in Fig. 7(b). The action spectra show the sensitization of zinc oxide by **20**, **21**, **22** and **23** at around 550 nm, whereas no sensitization was observed for **D131** at around 550 nm, as depicted in Fig. 7(c). The incident photon-to-current efficiency (IPCE) in the presence of CA was in the following dye order: **20** (83.1%) > **23** (78.2%), **D131** (77.8%) > **21** (69.1%) > **22** (55.5%) (Table 2, runs 1, 2, 4–6). The short-circuit photocurrent densities (J_{sc}) of **21** (8.15 mA cm^{-2}), **20** (8.09 mA cm^{-2}), **23** (7.42 mA cm^{-2}) and **22** (6.69 mA cm^{-2}) were higher than that of **D131** (5.55 mA cm^{-2}). The fill factor (ff) was lowered by introducing a thiophene unit. Consequently, the η value was in the following order of dyes:

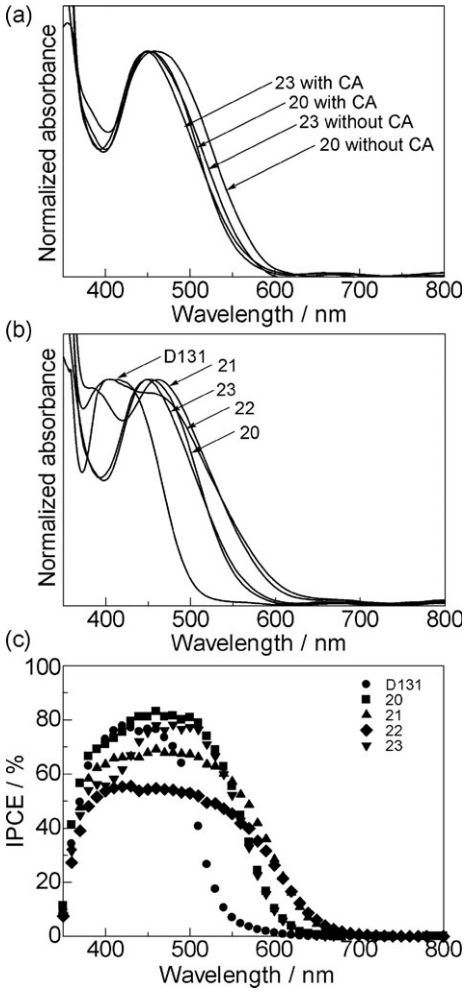

Fig. 7 (a) Normalized UV-vis absorption spectra of **20** and **23** on zinc oxide in the absence and presence of CA, (b) normalized UV-vis absorption spectra of **D131**, **20**, **21**, **22** and **23** on zinc oxide in the presence of CA and (c) action spectra of **D131**, **20**, **21**, **22** and **23** in the presence of CA.

20 (3.78%) > **23** (3.36%), **21** (3.19%) > **D131** (2.60%) > **22** (2.08%). Thus, an improvement in cell performance was successfully observed for a series of **D131**-type thiophene-conjugated indoline dyes. The improved cell performance of **20**, **21** and **23**, compared with **D131**, mainly came from the bathochromic shift in the absorption band and a high IPCE (>70%) to increase J_{sc}.

Next, the cell performance of **D102** and **24** was examined (Table 2, runs 8–10). The UV-vis absorption and action spectra are shown in Fig. 8. The absorption band of **24** was more bathochromic than that of **D102**. The absorption spectrum of **24** in the absence of CA clearly showed a broad absorption at around 600 nm, suggesting the formation of aggregates. Fig. 8(b) shows the sensitization of zinc oxide by **24** at around 630 nm. However, the IPCE value of **24** was lower than that of **D102** so as not to increase J_{sc}. The open-circuit voltage (V_{oc}) and ff of **24** were lower than those of **D102** (Table 2, runs 8 and 9). Thus, no improvement in cell performance was observed for **D102**-type thiophene-conjugated indoline dyes.

Table 2 Physical properties of indoline dyes

Run	Compound	CA[a]	λ_{max}/nm	Abs.[b]	IPCE (%)	J_{sc}/mA cm^{-2}	V_{oc}/V	ff	η[c] (%)
1	**D131**	2	405	3.36	77.8	5.55	0.66	0.71	2.60
2	**20**	2	449	2.48	83.1	8.09	0.69	0.68	3.78
3	**20**	0	459	1.96	71.4	7.09	0.65	0.68	3.13
4	**21**	2	461	2.16	69.1	8.15	0.63	0.62	3.19
5	**22**	2	457	2.44	55.5	6.69	0.59	0.53	2.08
6	**23**	2	450	2.07	78.2	7.42	0.66	0.68	3.36
7	**23**	0	452	2.07	76.2	7.58	0.65	0.67	3.30
8	**D102**	2	476	3.20	77.1	9.00	0.65	0.66	3.88
9	**24**	2	514	1.94	48.6	7.33	0.62	0.63	2.83
10	**24**	0	539	1.54	42.4	6.44	0.59	0.58	2.20
11	**D149**	2	521	3.08	81.2	11.08	0.68	0.57	4.23
12	**25**	2	547	1.76	43.4	6.85	0.54	0.64	2.35
13	**25**	0	555	1.65	35.9	5.38	0.50	0.62	1.68
14	**26**	2	546	1.25	37.5	5.85	0.62	0.68	2.45
15	**26**	0	561	1.21	37.7	5.55	0.57	0.65	2.07
16	**27**	2	546	1.26	29.7	4.40	0.59	0.66	1.71
17	**28**	2	542	1.45	26.1	3.67	0.56	0.67	1.36

[a] Equivalents of cholic acid with respect to dye. [b] Absorbance at absorption maximum on zinc oxide. [c] Action spectra and *I–V* characteristics under AM 1.5 irradiation (100 mW cm^{-2}).

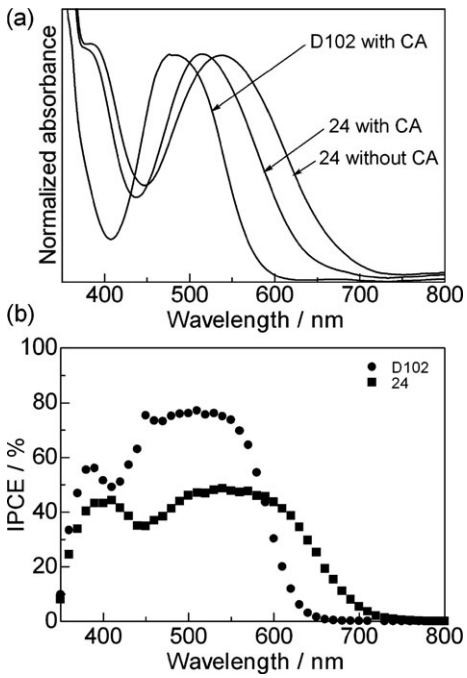

Fig. 8 (a) Normalized UV-vis absorption spectra of **D102** and **24** on zinc oxide in the absence and presence of CA, and (b) action spectra of **D102** and **24** in the presence of CA.

Finally, the cell performance of **D149**-type indoline dyes was examined. The UV-vis absorption and action spectra of **D149**, **25**, **26**, **27** and **28** are shown in Fig. 9. In this case, the difference in the UV-vis absorption bands of **25** and **26** in the absence and presence of CA was small compared with those in the cases of **20** and **23**, as shown in Fig. 9(a). The η values of **25** and **26** in the presence of CA were higher than those in the absence of CA (Table 2, runs 12–15). Fig. 9(b) shows that **25**, **26**, **27** and **28** are more bathochromic than **D149**. Fig. 9(c) indicates that though the sensitization of zinc oxide was observed for **25**, **26**, **27** and **28** at around 670 nm,

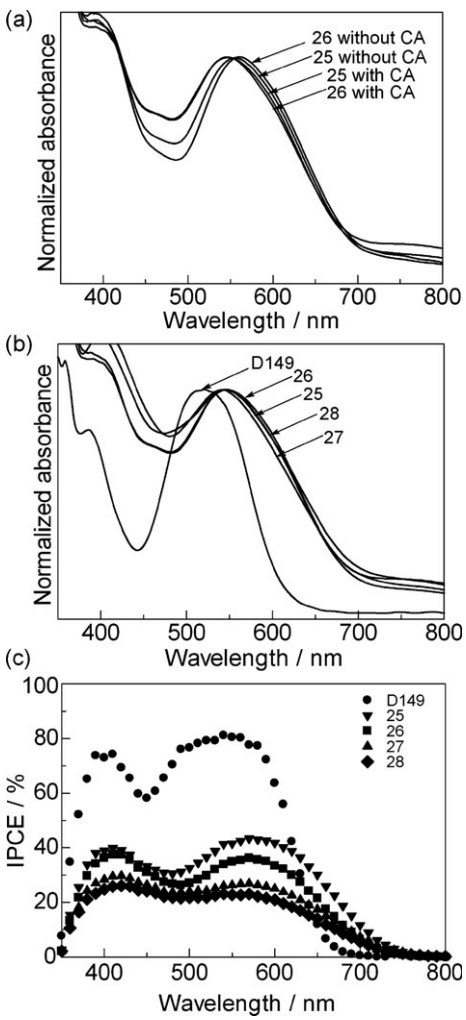

Fig. 9 (a) Normalized UV-vis absorption spectra of **25** and **26** on zinc oxide in the absence and presence of CA, (b) normalized UV-vis absorption spectra of **D149**, **25**, **26**, **27** and **28** on zinc oxide in the presence of CA, and (c) action spectra of **D149**, **25**, **26**, **27** and **28** in the presence of CA.

their IPCE values were lower than that of **D149**. Thus, no improvement in cell performance was observed for the series of **D149**-type thiophene-conjugated indoline dyes (Table 2, runs 11, 12, 14, 16 and 17).

Relationship between IPCE and E_{ox}, $E_{ox} - E_{0-0}$

To examine why only **D131**-type thiophene-conjugated indoline dyes showed improved cell performances, the relationship between IPCE and energy levels was examined. Fig. 10(a) shows the relationship between IPCE and E_{ox}. Indoline dyes **D131**, **20**, **21**, **23**, **D102** and **D149**, of which the E_{ox} levels were more positive than the *ca.* +0.25 V *vs.* Fc/Fc^+ in acetonitrile, showed high (>70%) IPCE values. The potential level of I^-/I_3^- was observed at −0.04 V *vs.* Fc/Fc^+ in acetonitrile. Fig. 10(b) shows the relationship between IPCE and $E_{ox} - E_{0-0}$. It was also found that indoline dyes **D131**, **20**, **21**, **23**, **D102** and **D149** showed high IPCE values. It is reported that the potential levels of the conduction band of titanium oxide and the I^-/I_3^- redox are −0.5 and +0.4 V *vs.* NHE, respectively, there being an energy gap of 0.9 V.[9,11] The conduction band level of zinc oxide is similar to that of titanium oxide. Therefore, the level of zinc oxide is considered to be −0.94 V *vs.* Fc/Fc^+ in acetonitrile, which is much more positive than the $E_{ox} - E_{0-0}$ levels of all the indoline dyes, the energy gap between $E_{ox} - E_{0-0}$ and the conduction band levels being larger than 0.7 V. It is suggested that an energy gap larger than 0.2 V between E_{ox} and I^-/I_3^-, and $E_{ox} - E_{0-0}$ and the conduction band levels, respectively, are required.[9] Thus, though the $E_{ox} - E_{0-0}$ level of all the indoline dyes are sufficiently negative, their E_{ox} levels are critical for the sensitization cycle to proceed. No marked difference in the E_{ox} levels among the thiophene-conjugated derivatives **20** (+0.25 V), **21** (+0.23 V), **22** (+0.22 V), **23** (+0.25 V), **24** (+0.25 V) and **25** (+0.24 V) was observed in solution. However, their E_{ox} level on zinc oxide could differ from that in solution. As the E_{ox} level of **D131** (+0.41 V *vs.* Fc/Fc^+ in MeCN) was more positive than those of **D102** (+0.37 V) and **D149** (+0.30 V) in solution, those of **D131**-type derivatives **20**, **21**, **22** and **23** might be more positive than those of **D102**- and **D149**-type derivatives **24**, **25**, **26**, **27** and **28** on zinc oxide. The E_{ox} levels of **D102**, **20**, **21** and **22** were observed at +0.37, +0.25, +0.23 and +0.22 V *vs.* Fc/Fc^+ in acetonitrile, respectively. This suggests that the E_{ox} level can negatively shift with increasing numbers of thiophene units on zinc oxide. Therefore, the E_{ox} levels of **D131**-type mono- and dithiophene derivatives **20**, **21** and **23** could be more positive than those of **D102**- and **D149**-type derivatives, and the redox potential of I^-/I_3^- on zinc oxide could show an improved cell performance. As a result, indoline dyes **20**, **21** and **23** could show better performances than **D131** due to larger J_{sc} values. The E_{ox} levels of **D102**- and **D149**-type thiophene-conjugated indoline dyes **24**, **25**, **26**, **27** and **28** might be too negative on zinc oxide, despite their bathochromic shift in the UV-vis absorption spectrum on zinc oxide. In order to improve the performance of indoline dyes, it is important to design derivatives of them having more positive E_{ox} level.

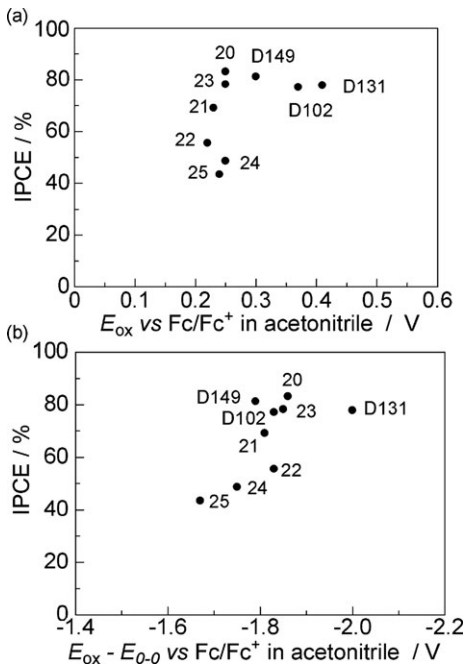

Fig. 10 The relationship between IPCE and energy levels: (a) IPCE *vs.* E_{ox} and (b) IPCE *vs.* $E_{ox} - E_{0-0}$.

Conclusion

A series of **D131**-, **D102**- and **D149**-type thiophene-conjugated indoline dyes were examined as sensitizers for zinc oxide solar cells, prepared by the one-step cathode deposition template method. Among the series of thiophene-conjugated indoline dyes, **D131**-type indoline dyes improved cell performance. This could have been due to their positive E_{ox} levels. In order to improve the performance of **D102**- and **D149**-type indoline dyes, it is important to design derivatives of them having more positive E_{ox} levels.

Experimental

General

Melting points were measured with a Yanagimoto MP-52 micro-melting-point apparatus. NMR spectra obtained using a JEOL JNM-ECX 400P spectrometer. EI and FAB MS spectra were recorded on a JEOL MStation 700 spectrometer. UV-vis absorption and fluorescence spectra were acquired on Hitachi U-3500 and F-4500 spectrophotometers, respectively. Cyclic voltammetry was carried out using an EG&G Princeton Applied Research Potentiostat/Galvanostat (Model 263A) driven by the M270 software package. One-step cathode electrodeposition was undertaken using a Hokuto-Denko HSV-100 potentiostat system. The photoelectrochemical measurements of solar cells were performed on a Bunko-Keiki CEP-2000 system. The *I–V* curve measurements of solar cells were performed on an EKO Instruments *I–V* curve tracer MP-160 and Grating spectroradiometer LS-100.

Electrochemical measurements

The electrochemical measurements of indoline dyes **D131**, **20**, **21**, **22**, **23**, **D102**, **24**, **D149**, **25**, ferrocene and potassium

iodide, were performed in acetonitrile. The oxidation potential (E_{ox}) was measured by using three small-sized electrodes. Ag/Ag^+ was used as a reference electrode. Platinum wire was used as the working and counterelectrode. Acetonitrile solutions (2 ml) of dyes containing tetrabutylammonium perchlorate (0.1 mol dm^{-3}) were prepared. Dry argon gas was introduced into the solution for 10 min. The electrochemical measurements were then performed at a scan rate of 100 mV s^{-1}.

Preparation of the zinc oxide solar cell

An aqueous potassium chloride solution (300 ml, 0.1 mol dm^{-3}) was electrolyzed at −1.0 V *vs.* SCE with bubbling oxygen gas at 70 °C for 30 min. Platinum was used as a counterelectrode. To the pre-electrolyzed film was added an aqueous solution of zinc chloride. The concentration of zinc chloride was adjusted to 5 mmol dm^{-3}. Then, the film was again electrodeposited in the solution at −1.0 V *vs.* SCE at 70 °C for 20 min with bubbling oxygen gas. To the electrodeposited film was added an aqueous solution of eosin Y (0.050 mmol dm^{-3}). The film was electrodeposited at −1.0 V *vs.* SCE at 70 °C for 30 min with bubbling oxygen gas. The film was kept in a dilute aqueous potassium hydroxide solution (pH 10.5) for 24 h to remove adsorbed eosin Y. The film was then dried at 100 °C for 1 h. The thin film was immersed in a chloroform solution of dye (1×10^{-4} mol dm^{-3}) and kept at ambient temperature for 1 h to adsorb dyes **20–28** onto the zinc oxide. In the cases of **D131**, **D102** and **D149**, the film was immersed in an acetonitrile–*tert*-butyl alcohol 1 : 1 mixed solution (0.5 mmol dm^{-3}). Then, the film was washed with chloroform. In the cases of **D131**, **D102** and **D149**, the film was washed with an acetonitrile–*tert*-butyl alcohol 1 : 1 mixed solution. The films were dried under an air atmosphere at ambient temperature. The film was used as the working electrode. A platinum spattered film was used as the counterelectrode. The cell size was 5.0 × 5.0 mm. Thermosetting resin was put around the cell. An acetonitrile–ethylene carbonate (v/v = 1 : 4) mixed solution containing tetrabutylammonium iodide (0.5 mol dm^{-3}) and iodine (0.05 mol dm^{-3}) was used as the electrolyte.

Photoelectrochemical measurements

Action spectra were measured under monochromatic light with a constant photon number (5×10^{15} photon cm^{-2} s^{-1}). *I–V* characteristics were measured under illumination with AM 1.5 simulated sun light (100 mW cm^{-2}) through a shading mask (5.0 × 4.0 mm).

Synthesis of dyes

Materials. 1,2,3,3*a*,4,8*b*-Hexahydro-4-[4-(2,2-diphenylethenyl)-phenyl]cyclopent[*b*]indole (**1**) was supplied from Chemicrea Co. Ltd. *N*-Bromosuccinimide (NBS, **2**) and 2-(4,4,5,5-tetramethyl-1,3,2-dioxaborolan-2-yl)thiophene (**4**) were purchased from Wako Pure Chemical Industries Ltd. 5-(4,4,5,5-Tetramethyl-1,3,2-dioxaborolan-2-yl)-2,2′-bithiophene (**5**), 5-(4,4,5,5-tetramethyl-1,3,2-dioxaborolan-2-yl)-2,2′,5′,2″-terthiophene (**6**) and cyano acetic acid (**16**) were purchased from Aldrich Co. Ltd. Rhodanine-3-acetic acid (**17**) was purchased from Tokyo Kasei Co. Ltd. Compound **19** was synthesized in the similar procedure to that described for **18**.[12] 3-Hexyl-2-(4,4,5,5-tetramethyl-1,3,2-dioxaborolan-2-yl)thiophene (**7**)[13] and 3,5-(di-*tert*-butyl)benzylamine[14] were synthesized as described in the literature. **D131**, **D102** and **D149** were prepared in a similar way, as described in the literature.[5c,e]

Synthesis of 3. To a dry acetone solution (23 ml) of **1** (980 mg, 2.37 mmol) was added NBS (423 mg, 2.38 mmol) at 0 °C under an argon atmosphere. The mixture was stirred at room temperature for 3 h. The reaction mixture was poured into water (20 ml) and extracted with chloroform (3 × 50 ml). The extract was washed with brine (2 × 50 ml) and dried over anhydrous sodium sulfate. The solvent was removed *in vacuo*. The crude product was purified by silica gel column chromatography (chloroform–hexane = 1 : 3) to afford **3** as a pale yellow solid. Yield 96%, mp 81–83 °C. δ_H (400 MHz, $CDCl_3$, Me_4Si): 1.42–1.49 (1 H, m), 1.61–1.65 (1 H, m), 1.79–1.87 (3 H, m), 1.96–2.02 (1 H, m), 3.76–3.79 (1 H, m), 4.65–4.69 (1 H, m), 6.83 (1 H, d, J = 8.4 Hz), 6.92 (1 H, s), 6.99–7.01 (4 H, m), 7.09 (1 H, d, J = 8.4 Hz), 7.16 (1 H, s) and 7.24–7.40 (10 H, m). m/z (EI) = 493 (M^+ + 2, 100), 491 (M^+, 98), 464 (69), 462 (67), 413 (55), 384 (52) and 178 (42).

Synthesis of 8–11. To a THF solution (10 ml) of **3** (492 mg, 1.0 mmol) were added boronic acid esters **4–7** (1.20 mmol), tetrakis(triphenylphosphine)palladium(0) (60 mg, 0.05 mmol) and a 2 M aqueous potassium carbonate solution (0.8 ml). The mixture was refluxed (**8**: 12 h, **9**: 20 h, **10**: 20 h and **11**: 20 h) under an argon atmosphere. After cooling, chloroform (100 ml) was added to the reaction mixture and it was then filtered through Celite. The filtrate was next poured into water (50 ml). The chloroform layer was washed with brine (3 × 50 ml) and dried over anhydrous sodium sulfate. The solvent was removed *in vacuo* and the crude product purified by silica gel column chromatography (**8**: chloroform–hexane = 4 : 3 × 1, chloroform × 1; **9**: chloroform–hexane = 1 : 1 × 1, chloroform–hexane = 2 : 5 × 1; **10**: chloroform–hexane = 1 : 1 × 1, chloroform–hexane = 3 : 5 × 2; **11**: chloroform–hexane = 8 : 11 × 1, chloroform–hexane = 1 : 3 × 2) to give **8–11** as a yellow solid. The physical and spectral data are shown below.

8. Yield 72%, mp 204–206 °C. δ_H (400 MHz, $CDCl_3$, Me_4Si): 1.46–1.51 (1 H, m), 1.62–1.67 (1 H, m), 1.79–1.94 (3 H, m), 2.00–2.07 (1 H, m), 3.81–3.86 (1 H, m), 4.70–4.73 (1 H, m), 6.93 (1 H, s), 6.98–7.06 (6 H, m), 7.15 (1 H, s), 7.16–7.17 (1 H, m) and 7.26–7.39 (12 H, m). m/z (EI) = 495 (M^+, 100), 466 (24) and 248 (8).

9. Yield 49%, mp 105–107 °C. δ_H (400 MHz, $CDCl_3$, Me_4Si): 1.39–1.47 (1 H, m), 1.55–1.59 (1 H, m), 1.69–1.84 (3 H, m), 1.91–2.00 (1 H, m), 3.69–3.73 (1 H, m), 4.58–4.61 (1 H, m), 6.91–7.03 (8 H, m), 7.08–7.10 (3 H, m) and 7.21–7.34 (12 H, m). m/z (FAB) = 578 (MH^+).

10. Yield 53%, mp 106–109 °C. δ_H (400 MHz, $CDCl_3$, Me_4Si): 1.48–1.59 (1 H, m), 1.62–1.66 (1 H, m), 1.82–1.93 (3 H, m), 2.03–2.06 (1 H, m), 3.80–3.88 (1 H, m), 4.67–4.78 (1 H, m), 6.94 (1 H, s), 6.98–7.11 (10 H, m), 7.17 (1 H, d,

J = 3.4 Hz), 7.21 (1 H, d, J = 4.8 Hz) and 7.27–7.41 (12 H, m). m/z (FAB) = 660 (MH^+).

11. Yield 56%, mp 57–61 °C. δ_H (400 MHz, $CDCl_3$, Me_4Si): 0.89 (3 H, t, J = 6.8 Hz), 1.30–1.34 (6 H, m), 1.42–1.52 (1 H, m), 1.59–1.64 (3 H, m), 1.78–1.90 (3 H, m), 1.97–2.07 (1 H, m), 2.58 (2 H, t, J = 7.6 Hz), 3.78–3.82 (1 H, m), 4.66–4.69 (1 H, m), 6.73 (1 H, s), 6.92–7.04 (7 H, m) and 7.22–7.40 (12 H, m). m/z (FAB) = 580 (MH^+).

Synthesis of 12–15. To DMF (4 ml) was added phosphorous oxychloride (352 mg, 2.30 mmol) at 0 °C. To the solution was then added a DMF solution (14 ml) of **8–11** (0.84 mmol) at 0–5 °C. The mixture was heated at 75 °C (**12**: 2 h, **13**: 4 h, **14**: 20 h and **15**: 2 h). After the reaction was complete, the reaction mixture was poured into ice–water (100 ml) and neutralized with aqueous sodium hydroxide. The product was extracted with chloroform (3 × 50 ml). The extract was washed with brine (2 × 50 ml) and water (2 × 50 ml), and dried over anhydrous sodium sulfate. The solvent was removed *in vacuo* and the product purified by silica gel column chromatography (2 × chloroform) to afford **12–15** (**12**: orange solid, **13**: red solid, **14**: red solid and **15**: orange solid). The physical and spectral data are shown below.

12. Yield 90%, mp 112–114 °C. δ_H (400 MHz, $CDCl_3$, Me_4Si): 1.47–1.53 (1 H, m), 1.65–1.67 (1 H, m), 1.82–1.89 (3 H, m), 2.07–2.11 (1 H, m), 3.81–3.85 (1 H, m), 4.76–4.79 (1 H, m), 6.94 (1 H, s), 6.96 (1 H, d, J = 8.5 Hz), 7.01 (2 H, d, J = 8.8 Hz), 7.05 (2 H, d, J = 8.8 Hz), 7.23–7.39 (13 H, m), 7.68 (1 H, d, J = 4.1 Hz) and 9.80 (1 H, s). m/z (EI) = 523 (M^+, 100), 495 (56), 373 (52) and 344 (31).

13. Yield 74%, mp 115–117 °C. δ_H (400 MHz, $CDCl_3$, Me_4Si): 1.44–1.53 (1 H, m), 1.59–1.66 (1 H, m), 1.77–1.91 (3 H, m), 2.00–2.09 (1 H, m), 3.79–3.81 (1 H, m), 4.70–4.73 (1 H, m), 6.93 (1 H, s), 6.95 (1 H, d, J = 8.5 Hz), 6.99 (2 H, d, J = 8.9 Hz), 7.03 (2 H, d, J = 8.9 Hz), 7.08 (1 H, d, J = 3.9 Hz), 7.18 (1 H, d, J = 3.9 Hz), 7.24–7.40 (13 H, m), 7.62 (1 H, d, J = 4.1 Hz) and 9.82 (1 H, s). m/z (FAB) = 606 (MH^+).

14. Yield 26%, mp 230–232 °C. δ_H (400 MHz, $CDCl_3$, Me_4Si): 1.46–1.54 (1 H, m), 1.62–1.68 (1 H, m), 1.79–1.86 (3 H, m), 1.98–2.02 (1 H, m), 3.77–3.99 (1 H, m), 4.46–4.69 (1 H, m), 6.38–7.40 (23 H, m), 7.57–7.58 (1 H, m) and 9.78 (1 H, s). m/z (FAB) = 688 (MH^+).

15. Yield 96%, mp 66–68 °C. δ_H (400 MHz, $CDCl_3$, Me_4Si): 0.89 (3 H, t, J = 7.0 Hz), 1.30–1.39 (6 H, m), 1.45–1.48 (1 H, m), 1.61–1.73 (3 H, m), 1.79–1.90 (3 H, m), 2.02–2.05 (1 H, m), 2.91 (2 H, t, J = 7.0 Hz), 3.79–3.83 (1 H, m), 4.73–4.77 (1 H, m), 6.93 (1 H, s), 6.94 (1 H, d, J = 8.2 Hz), 7.00 (2 H, d, J = 8.9 Hz), 7.04 (2 H, d, J = 8.9 Hz), 7.06 (1 H, s), 7.23–7.40 (12 H, m) and 9.95 (1 H, s). m/z (FAB) = 608 (MH^+).

Synthesis of 20, 21, 22 and 23. In the cases of **20**, **21** and **23**, to an acetonitrile solution (6 ml) of **12**, **13** and **14** (0.30 mmol) were added cyano acetic acid (100 mg, 1.18 mmol) and piperidine (46 mg, 0.54 mmol). In the case of **22**, to an acetonitrile–chloroform (1 : 1) mixed solution (80 ml) of **14** (107 mg, 0.16 mmol) were added cyano acetic acid (97 mg, 1.14 mmol) and piperidine (776 mg, 9.11 mmol). The mixture was then refluxed (**20**: 2 h, **21**: 2 h, **22**: 23 h and **23**: 17 h). After cooling, the solvent was removed *in vacuo* and the residue dissolved in chloroform. To the solution was added 1 M aqueous hydrochloric acid (0.4 ml) and water (50 ml), and the mixture stirred at room temperature for 30 min. The chloroform layer was separated, washed with water (3 × 50 ml) and dried over anhydrous sodium sulfate. The solvent was removed *in vacuo* and the product purified by silica gel column chromatography (**20**: chloroform–methanol = 8 : 1 × 1, 10 : 1 × 2; **21**: chloroform–methanol = 10 : 1 × 3; **22**: chloroform–methanol = 10 : 1 × 1, 8 : 1 × 3; **23**: chloroform–methanol = 10 : 1 × 3) to afford **20**, **21**, **22** and **23** as a purple solid. The physical and spectral data are shown below.

20. Yield 64%, mp 268–271 °C. δ_H (400 MHz, DMSO-d_6, Me_4Si): 1.23–1.32 (1 H, m), 1.59–1.68 (2 H, m), 1.79–1.84 (2 H, m), 1.99–2.08 (1 H, m), 3.82–3.86 (1 H, m), 4.86–4.90 (1 H, m), 6.97 (1 H, d, J = 8.7 Hz), 7.02 (2 H, d, J = 8.5 Hz), 7.07 (1 H, s), 7.11 (2 H, d, J = 8.5 Hz), 7.19–7.22 (2 H, m), 7.28–7.36 (5 H, m), 7.41–7.48 (4 H, m), 7.57–7.59 (2 H, m), 7.95 (1 H, d, J = 3.4 Hz) and 8.43 (1 H, s). m/z (FAB) = 591.2106 (MH^+, $C_{39}H_{31}N_2O_2S$ requires 591.2106).

21. Yield 62%, mp 194–198 °C. δ_H (400 MHz, DMSO-d_6, Me_4Si): 1.28–1.35 (1 H, m), 1.58–1.69 (2 H, m), 1.81–1.86 (2 H, m), 2.00–2.07 (1 H, m), 3.81–3.85 (1 H, m), 4.81–4.84 (1 H, m), 6.98 (1 H, d, J = 9.2 Hz), 7.00 (2 H, d, J = 9.1 Hz), 7.06 (1 H, s), 7.09 (2 H, d, J = 9.1 Hz), 7.20–7.21 (2 H, m), 7.28–7.53 (13 H, m), 7.82 (1 H, br s) and 8.28 (1 H, br s). m/z (FAB) = 673.1974 (MH^+, $C_{43}H_{33}N_2O_2S_2$ requires 673.1983).

22. Yield 79%, mp 266–269 °C. δ_H (400 MHz, DMSO-d_6, Me_4Si): 1.29–1.36 (1 H, m), 1.61–1.70 (2 H, m), 1.84–1.87 (2 H, m), 2.00–2.05 (1 H, m), 3.81–3.85 (1 H, m), 4.80–4.83 (1 H, m), 6.98 (1 H, d, J = 6.3 Hz), 7.00 (2 H, d, J = 7.8 Hz), 7.06 (1 H, s), 7.08 (2 H, d, J = 7.8 Hz), 7.20–7.22 (2 H, m), 7.28–7.47 (13 H, m), 7.60–7.62 (2 H, m), 7.98 (1 H, d, J = 3.4 Hz) and 8.49 (1 H, s). m/z (FAB) = 755.1831 (MH^+, $C_{47}H_{35}N_2O_2S_3$ requires 755.1861).

23. Yield 93%, mp 240–243 °C. δ_H (400 MHz, DMSO-d_6, Me_4Si): 0.84 (3 H, t, J = 6.0 Hz), 1.20–1.30 (7 H, m), 1.57–1.65 (4 H, m), 1.76–1.84 (2 H, m), 1.97–2.06 (1 H, m), 2.74 (2 H, t, J = 7.2 Hz), 3.78–3.82 (1 H, m), 4.82–4.86 (1 H, m), 6.93 (1 H, d, J = 8.2 Hz), 6.99 (2 H, d, J = 8.6 Hz), 7.04 (1 H, s), 7.07 (2 H, d, J = 8.6 Hz), 7.17–7.19 (2 H, m), 7.26–7.34 (5 H, m), 7.38–7.45 (4 H, m), 7.50 (1 H, s), 7.54 (1 H, s) and 8.25 (1 H, s). m/z (FAB) = 675.3117 (MH^+, $C_{45}H_{43}N_2O_2S$ requires 675.3045).

Synthesis of 24, 25, 26, 27 and 28. To an acetic acid solution (4 ml) of **12–14** (0.30 mmol) was added rhodanine derivatives **17–19** (0.32 mmol). The mixture was heated at 120 °C and ammonium acetate (0.88 mmol) added, after which it was refluxed for 2 h. After cooling, the reaction mixture was poured into water (20 ml). The resulting precipitate was filtered and washed with water, and the crude product purified by silica gel column chromatography (**24**: chloroform–methanol = 8 : 1 × 3; **25**: chloroform–methanol = 8 : 1 × 2; **26**:

chloroform–methanol = 8 : 1 × 9; **27**: chloroform–methanol = 8 : 1 × 5; **28**: chloroform–methanol = 8 : 1 × 3) to afford compound **24**, **25**, **26**, **27** and **28** as a purple solid. The physical and spectral data are shown below.

24. Yield 89%, mp 175–178 °C. δ_H (400 MHz, DMSO-d_6, Me_4Si): 1.29–1.33 (1 H, m), 1.59–1.68 (2 H, m), 1.81–1.84 (2 H, m), 2.00–2.05 (1 H, m), 3.81–3.85 (1 H, m), 4.69 (2 H, s), 4.84–4.88 (1 H, m), 6.95 (1 H, d, J = 8.5 Hz), 7.01 (2 H, d, J = 8.3 Hz), 7.06 (1 H, s), 7.09 (2 H, d, J = 8.3 Hz), 7.19–7.21 (2 H, m), 7.28–7.34 (5 H, m), 7.39–7.49 (4 H, m), 7.57–7.58 (2 H, m), 7.77 (1 H, d, J = 3.9 Hz) and 8.10 (1 H, s). m/z (FAB) = 697.1647 (MH^+, $C_{41}H_{33}N_2O_3S_3$ requires 697.1653).

25. Yield 31%, mp > 300 °C. δ_H (400 MHz, DMSO-d_6, Me_4Si): 1.14 (3 H, t, J = 6.9 Hz), 1.25–1.37 (1 H, m), 1.60–1.68 (2 H, m), 1.80–1.84 (2 H, m), 2.01–2.08 (1 H, m), 3.82–3.86 (1 H, m), 3.98–4.00 (2 H, m), 4.69 (2 H, s), 4.84–4.87 (1 H, m), 6.96 (1 H, d, J = 8.5 Hz), 7.00 (2 H, d, J = 9.3 Hz), 7.07 (1 H, s), 7.08 (2 H, d, J = 9.3 Hz), 7.20–7.55 (13 H, m), 7.68 (1 H, d, J = 3.9 Hz) and 8.02 (1 H, s). m/z (FAB) = 824.1757 (MH^+, $C_{46}H_{38}N_3O_4S_4$ requires 824.1745).

26. Yield 81%, mp > 300 °C. δ_H (400 MHz, DMSO-d_6, Me_4Si): 1.24–1.29 (1 H, m), 1.25 (18 H, s), 1.59–1.87 (2 H, m), 1.85–1.87 (2 H, m), 2.01–2.09 (1 H, m), 3.83–3.87 (1 H, m), 4.61 (2 H, s), 4.85–4.88 (1 H, m), 5.19 (2 H, s), 6.98 (1 H, d, J = 8.5 Hz), 7.00 (2 H, d, J = 8.8 Hz), 7.07 (1 H, m), 7.10 (2 H, d, J = 8.8 Hz), 7.19–7.48 (14 H, m), 7.53 (1 H, s), 7.57 (1 H, d, J = 3.9 Hz), 7.72 (1 H, d, J = 4.1 Hz) and 8.07 (1 H, s). m/z (FAB) = 998.3133 (MH^+, $C_{59}H_{56}N_3O_4S_4$ requires 998.3154).

27. Yield 95%, mp > 300 °C. δ_H (400 MHz, DMSO-d_6, Me_4Si): 1.22–1.35 (1 H, m), 1.23 (18 H, s), 1.57–1.66 (2 H, m), 1.78–1.85 (2 H, m), 1.95–2.05 (1 H, m), 3.73–3.79 (1 H, m), 4.33 (2 H, s), 4.74–4.78 (1 H, m), 5.10 (2 H, s), 6.91 (1 H, d, J = 8.5 Hz), 6.99 (2 H, d, J = 8.3 Hz), 7.03 (1 H, s), 7.04 (2 H, d, J = 8.3 Hz), 7.17–7.54 (18 H, m), 7.62 (1 H, s) and 7.94 (1 H, s). m/z (FAB) = 1080.3016 (MH^+, $C_{63}H_{58}N_3O_4S_5$ requires 1080.3031).

28. Yield 32%, mp > 300 °C. δ_H (400 MHz, DMSO-d_6, Me_4Si): 1.22–1.33 (1 H, m), 1.26 (18 H, s), 1.59–1.68 (2 H, m), 1.80–1.84 (2 H, m), 1.97–2.03 (1 H, m), 3.78–3.83 (1 H, m), 4.46 (2 H, s), 4.77–4.81 (1 H, m), 5.17 (2 H, s), 6.96 (1 H, d, J = 8.5 Hz), 6.98 (2 H, d, J = 9.1 Hz), 7.05 (1 H, s), 7.06 (2 H, d, J = 9.1 Hz), 7.19–7.54 (20 H, m), 7.71 (1 H, s) and 8.02 (1 H, s). m/z (FAB) = 1162.2795 (MH^+, $C_{67}H_{60}N_3O_4S_6$ requires 1162.2908).

Acknowledgements

This work was financially supported in part by Grants-in-Aid for Science Research (no. 19550185) from the Japan Society for the Promotion of Science (JSPS).

References

1 (*a*) Z.-S. Wang, K. Hara, Y. Dan-oh, C. Kasada, A. Shinpo, S. Suga, H. Arakawa and H. Sugihara, *J. Phys. Chem. B*, 2005, **109**, 3907; (*b*) K. Hara, M. Kurashige, Y. Dan-oh, C. Kasada, A. Shinpo, S. Suga, K. Sayama and H. Arakawa, *New J. Chem.*, 2003, **27**, 783; (*c*) K. Hara, K. Sayama, Y. Ohga, A. Shinpo, S. Suga and H. Arakawa, *Chem. Commun.*, 2001, 569.

2 (*a*) T. Dentani, K. Nagasaka, K. Funabiki, J.-Y. Jin, T. Yoshida, H. Minoura and M. Matsui, *Dyes Pigm.*, 2008, **77**, 59; (*b*) Q.-H. Yao, L. Shan, F.-Y. Li, D.-D. Yin and C.-H. Huang, *New J. Chem.*, 2003, **27**, 1277; (*c*) Z.-S. Wang, F.-Y. Li and C.-H. Huang, *J. Phys. Chem. B*, 2001, **105**, 9210; (*d*) Z.-S. Wang, F.-Y. Li, C.-H. Huang, L. Wang, M. Wei, L.-P. Jim and N.-Q. Li, *J. Phys. Chem. B*, 2000, **104**, 9676; (*e*) Z.-S. Wang, F.-Y. Li and C.-H. Huang, *Chem. Commun.*, 2000, 2063.

3 (*a*) R. Chen, X. Yang, H. Tian and L. Sun, *J. Photochem. Photobiol., A*, 2007, **189**, 295; (*b*) M. Liang, W. Xu, F. Cai, P. Chen, B. Peng, J. Chen and Z. Li, *J. Phys. Chem. C*, 2007, **111**, 4465; (*c*) H. Choi, J.-K. Lee, K.-J. Song, K. Song, S. O. Kang and J. Ko, *Tetrahedron*, 2007, **63**, 1553; (*d*) N. Koumura, Z.-S. Wang, S. Mori, M. Miyashita, E. Suzuki and K. Hara, *J. Am. Chem. Soc.*, 2006, **128**, 14256; (*e*) S. Kim, J. K. Lee, S. O. Kang, J. Ko, J.-H. Yum, S. Fantacci, F. D. Angelis, D. D. Censo, M. K. Nazeeruddin and M. Grätzel, *J. Am. Chem. Soc.*, 2006, **128**, 16701; (*f*) D. P. Hagberg, T. Edvinsson, T. Marinado, G. Boschloo, A. Hagfeldt and L. Sun, *Chem. Commun.*, 2006, 2245; (*g*) K. Hara, T. Sato, R. Katoh, A. Furube, T. Yoshihara, M. Murai, M. Kurashige, S. Ito, A. Shinpo, S. Suga and H. Arakawa, *Adv. Funct. Mater.*, 2005, **15**, 246; (*h*) T. Kitamura, M. Ikeda, K. Shigaki, T. Inoue, N. A. Anderson, X. Ai, T.-Q. Lian and S. Yanagida, *Chem. Mater.*, 2004, **16**, 1806; (*i*) K. Hara, M. Kurashige, S. Ito, A. Shinpo, S. Suga, K. Sayama and H. Arakawa, *Chem. Commun.*, 2003, 252.

4 (*a*) D. Kim, J.-K. Lee, S. O. Kang and J. Ko, *Tetrahedron*, 2007, **63**, 1913; (*b*) I. Jung, J.-K. Lee, K.-H. Song, K. Song, S. O. Kang and J. Ko, *J. Org. Chem.*, 2007, **72**, 3652; (*c*) S. Kim, J.-K. Lee, S. O. Kang, J. Ko, J.-H. Yum, S. Fantacci, F. D. Angelis, D. D. Censo, M. K. Nazeeruddin and M. Grätzel, *J. Am. Chem. Soc.*, 2006, **128**, 16701.

5 (*a*) S. Ito, S. M. Zakeeruddin, R. Humphry-Baker, P. Liska, R. Charvet, P. Comte, M. K. Nazeeruddin, P. Pechy, M. Takata, H. Miura, S. Uchida and M. Grätzel, *Adv. Mater.*, 2006, **18**, 1202; (*b*) L. Schmidt-Mende, U. Bach, R. Humphry-Baker, T. Horiuchi, H. Miura, S. Ito, S. Uchida and M. Grätzel, *Adv. Mater.*, 2005, **17**, 813; (*c*) T. Horiuchi, H. Miura and S. Uchida, *J. Photochem. Photobiol., A*, 2004, **164**, 29; (*d*) T. Horiuchi, H. Miura, K. Sumioka and S. Uchida, *J. Am. Chem. Soc.*, 2004, **126**, 12218; (*e*) T. Horiuchi, H. Miura and S. Uchida, *Chem. Commun.*, 2003, 3036; (*f*) W. H. Howie, F. Claeyssens, H. Miura and L. M. Peter, *J. Am. Chem. Soc.*, 2008, **130**, 1367.

6 A. Otsuka, K. Funabiki, N. Sugiyama, T. Yoshida, H. Minoura and M. Matsui, *Chem. Lett.*, 2006, **35**, 666.

7 P. Y. Reddy, L. Giribabu, C. Lyness, H. J. Snaith, C. Vijaykumar, M. Chandrasekharam, M. Lakshmikantam, J.-H. Yum, K. Kalyanasundaram, M. Grätzel and M. K. Nazeeruddin, *Angew. Chem., Int. Ed.*, 2007, **46**, 373.

8 M. Matsui, Y. Hashimoto, K. Funabiki, J. Y. Jin, T. Yoshida and H. Minoura, *Synth. Met.*, 2005, **148**, 147.

9 K. Hara, T. Sato, R. Katoh, A. Furube, Y. Ohga, A. Shinpo, S. Suga, K. Sayama, H. Sugihara and H. Arakawa, *J. Phys. Chem. B*, 2003, **107**, 597.

10 T. Yoshida, M. Iwaya, H. Ando, T. Oekermann, K. Nonomura, D. Schlettwein, D. Wöhrle and H. Minoura, *Chem. Commun.*, 2004, 400.

11 R. Katoh, A. Furube, T. Yoshihara, K. Hara, G. Fujihashi, S. Takano, S. Murata, H. Arakawa and M. Tachiya, *J. Phys. Chem. B*, 2004, **108**, 4818.

12 J. D. Mee, *US Pat.*, 5679795, 1997.

13 G. Bidan, A. De Nicola, V. Enée and S. Guilerez, *Chem. Mater.*, 1998, **10**, 1052.

14 M. Matsui, M. Wang, K. Funabiki, Y. Hayakawa and T. Kitaguchi, *Dyes Pigm.*, 2007, **74**, 169.